

Temporal decoupling of spin and crystallographic phase transitions in $\text{Fe}(\text{ptz})_6(\text{BF}_4)_2$

Hiroshi Watanabe,¹ Hideki Hirori,² Gabor Molnár,^{3,4} Azzedine Bousseksou,^{3,4} and Koichiro Tanaka^{1,2,*}

¹*Department of Physics, Graduate School of Science, Kyoto University, Sakyo-ku, Kyoto 606-8502, Japan*

²*Institute for Integrated Cell-Material Sciences, Kyoto University, Sakyo-ku, Kyoto 606-8501, Japan*

³*Laboratoire de Chimie de Coordination, CNRS, 205 Route de Narbonne, 31077 Toulouse, France*

⁴*UPS, INPT, LCC, Université de Toulouse, F-31077 Toulouse, France*

(Received 15 April 2009; published 12 May 2009)

We have studied relaxation dynamics of the thermally and photoinduced metastable states in $[\text{Fe}(\text{ptz})_6](\text{BF}_4)_2$ near the spin transition temperature using magnetic-susceptibility measurements and optical-absorption spectroscopy as function of the time. We observed two-step relaxations from the photoinduced high-spin to the ground low-spin state. The time-resolved measurements of the spin-relaxation processes allow us to decouple the spin transition and the crystallographic phase transition and evaluate their intrinsic transition temperatures as 122 and 132 K, respectively.

DOI: 10.1103/PhysRevB.79.180405

PACS number(s): 75.30.Wx, 64.60.-i, 78.47.-p

The photoinduced phase-transition (PIPT) phenomenon has been extensively studied in a variety of systems because of its fundamental importance in physics and its potential applications in optical data storage and processing devices.¹⁻³ The cooperative interaction plays an important role in PIPT and induces nonlinear phenomena, such as the existence of a threshold light intensity and an incubation period.³⁻⁵ This is particularly true for iron(II) spin-crossover coordination complexes, where the photoirradiation causes a spin transition between the 5T_2 high-spin (HS) state and the 1A_1 low-spin (LS) state.

The thermal spin transition strongly coupled with the crystallographic phase transition is among the most intriguing phenomena in spin-crossover complexes.⁶⁻⁹ A delicate balance between two order parameters of spin and structure gives us possibilities to drive the materials into various metastable states by external stimuli. Even in other types of phase-transition phenomena in solids, e.g., the multiferroic systems,¹⁰ perovskite manganite,¹¹ prussian blue analogs,¹² and charge-transfer molecular crystals,^{13,14} the coupling and decoupling of charge, spin and lattice degrees of freedom are key matters for understanding and controlling of material phases. However, the strong coupling between different order parameters renders the respective phase-transition phenomena difficult to study, and direct selective observation of strongly coupled phase transitions is desirable. In systems which are described by several order parameters, time-resolved measurements may allow us to observe respective phase transitions from photoinduced metastable states to elucidate the underlying functional response.

In this Rapid Communication, we report the relaxation dynamics in the thermal-quenched and photoinduced HS (PIHS) states in the spin-crossover complex $[\text{Fe}(\text{ptz})_6](\text{BF}_4)_2$ near the thermal phase-transition temperature using time-resolved magnetic-susceptibility and optical-absorption spectroscopy measurements. $[\text{Fe}(\text{ptz})_6](\text{BF}_4)_2$ is well-established model system for studying the phase-transition phenomena with competing order parameters.^{7,8,15-22} We observed two-step relaxations in the PIHS state from the HS to LS state through an intermediate state. Using infrared (IR) spectroscopy we show that the intermediate state has the same spin and crystallographic structure as the quenched state. The temperature dependence of the HS fraction and the IR-

absorption spectra show that a spin transition without a crystallographic phase transition in the intermediate state should occur at 122 K. Furthermore, the critical slowing down phenomena indicates that the crystallographic phase transition with the spin transition occurs at 132 K.

Single crystals of $[\text{Fe}(\text{ptz})_6](\text{BF}_4)_2$ were prepared as described previously,²³ with a typical crystal size of $2 \times 2 \times 0.1$ mm. First, we made the magnetic-susceptibility χ measurement using a superconducting quantum interference device (SQUID) magnetometer (MPMS-5S Quantum Design), which has a 20 s time resolution. We estimated the HS fraction of the samples from the product of the magnetic susceptibility and temperature (χT).

Figure 1(a) shows the temperature dependence of the HS fraction on slow temperature change (1 K/min) and exhibits an abrupt thermal spin transition accompanied by a hysteresis loop. The spin transition temperatures (where the HS and LS fractions are equal to 0.5) upon heating $T_{1/2\uparrow}$ (LS \rightarrow HS) and cooling $T_{1/2\downarrow}$ (HS \rightarrow LS) are obtained as 137 and 125 K, respectively. The measured transition temperatures depend on the heating and cooling rate. It is known that this spin transition competes with a crystallographic phase transition.⁸ This compound exhibits two different crystallographic phases:¹⁶ rhombohedral at high temperature (HT) or a disordered phase at low temperature (LT). When the sample is cooled slowly (< 1 K/min), the HS \rightarrow LS spin transition is accompanied by a crystallographic phase transition from the HT to LT structure phase. On the contrary, quenching (> 10 K/min) to 80 K brings about the LS state without the crystallographic phase transition.

In order to elucidate the mechanism underlying the phase transitions with competing order parameters, we observed the relaxation dynamics of the HS fraction at various temperatures, as indicated by the lower arrows in Fig. 1(a). Figure 1(b) shows the relaxation curves of the HS fraction, γ_{HS} , from the upper branch of the hysteresis loop to the LS state, exhibiting a sigmoidal behavior. As shown in Fig. 1(b), the HS state relaxes to the LS state below 131 K and the relaxation time increases with increasing temperature. At 132 K, the initial HS fraction ($\gamma_{\text{HS}} = 0.85$) is persistent over 20 h.

As shown in Fig. 1(b), the relaxation curves of the HS fraction can be observed well above 127 K. However, we

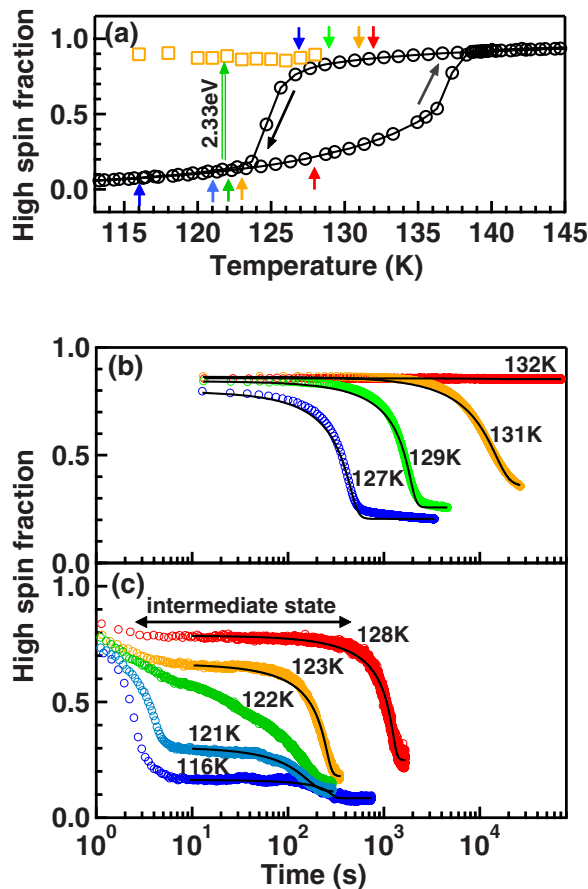


FIG. 1. (Color online) (a) Temperature dependence of the HS fraction obtained upon slow temperature change (1 K/min) (open circle) and the HS fraction in the PIHS state (open square) in $[\text{Fe}(\text{ptz})_6](\text{BF}_4)_2$ compound. (b) The relaxation curves from the HS state at the temperatures indicated by the lower arrows in Fig. 1(a): experimental results (open circle) and best-fit curves from Eq. (3) (solid line). (c) The relaxation curves from the PIHS state via the intermediate state in the dark at the temperatures indicated by the upper arrows in Fig. 1(a): experimental results (open circle) and best-fit curves from Eq. (3) (solid line).

cannot observe relaxation curves exactly below 127 K, because the relaxation time is less than a few minutes and the relaxation occurs before the temperature is stabilized. Moreover, the 20 s time resolution is insufficient to observe the relaxation process. To overcome this difficulty, we created the metastable HS states by laser irradiation and observed their relaxation dynamics by time-resolved optical-absorption spectroscopy.

The samples were excited using a frequency-doubled $\text{Nd}^{3+}:\text{YAG}$ laser (continuous wave, 2.33 eV, 3 W cm^{-2}). For measuring absorption spectra we used a halogen lamp as the probe light source and a Princeton Instruments spectrometer and charge coupled device (CCD) camera system (InSight100A), which has a 1 ms time resolution. The absorption spectra in the visible region for $[\text{Fe}(\text{ptz})_6](\text{BF}_4)_2$ have been assigned in Ref. 24. In the LS state, a broad absorption band is observed around 550 nm, corresponding to the $d-d$ transition from the 1A_1 to 1T_1 state. We estimated the HS fraction from the integrated area of optical densities from 500 to 650 nm.²⁴

We plot the temperature dependence of the HS fraction in the PIHS state with the open square symbols in Fig. 1(a). The PIHS state with a HS fraction of approximately 0.9 was created by 10 s laser irradiation. We confirmed that the HS state was not created by the laser heating effect but generated through photoexcitation by FTIR spectroscopy.²⁵ Figure 1(c) shows the relaxation dynamics of the PIHS state at various temperatures indicated by the upper arrows in Fig. 1(a). One can see two-step relaxation processes from the PIHS to ground LS state via an intermediate state. At 128 K, the spin state first relaxes to the intermediate state within a few seconds where it is stable for about 300 s before relaxing to the LS state with a sigmoidal behavior. Above 122 K, both the HS fraction in the intermediate state and its relaxation time decrease as the temperature decreases. At 122 K, the intermediate state almost disappears. Meanwhile, as the temperature decreases below 122 K, the intermediate state reappears and the relaxation time increases.

It is well known that the trapped HS state can be created in several iron(II) spin-crossover complexes by irradiating the ${}^1A_{1g} \rightarrow {}^1T_{1g}$ $d-d$ absorption band well below the thermal spin transition temperature. In many cases the relaxation dynamics of the PIHS state show sigmoidal curves.^{8,15} This nonexponential relaxation process is explained as the effect of cooperative interactions between the molecules. Hauser^{8,15} introduced an empirical model for the sigmoidal relaxation dynamics taking into account the self-acceleration process as follows:

$$\frac{d\gamma_{\text{HS}}}{dt} = -k(\gamma_{\text{HS}})\gamma_{\text{HS}}, \quad (1)$$

$$k(\gamma_{\text{HS}}) = k_0 \exp[\alpha(1 - \gamma_{\text{HS}})] = \frac{1}{\tau} \exp[\alpha(0.5 - \gamma_{\text{HS}})], \quad (2)$$

where $k(\gamma_{\text{HS}})$ is the relaxation rate, γ_{HS} is the HS fraction, and α is the acceleration factor. In conventional relaxation processes ($\alpha=0$), $k(\gamma_{\text{HS}})$ is independent of γ_{HS} , and the relaxation time is defined as the inverse of $k(\gamma_{\text{HS}})$. On the contrary, for relaxation processes showing a sigmoidal curve, the relaxation rate $k(\gamma_{\text{HS}})$ depends on the HS fraction, as described by Eq. (2). Hence, we define the relaxation time τ as an inverse of $k(\gamma_{\text{HS}})$ at $\gamma_{\text{HS}}=0.5$, i.e., $\tau = k_0^{-1} \exp(-0.5\alpha)$. Equation (1) leads the HS fraction to zero at the equilibrium state. However, the observed sigmoidal relaxation curves in Figs. 1(b) and 1(c) show that the HS fraction γ_f is not zero at the final state and moreover the initial HS fraction γ_i is not unity.²⁶ Therefore, we define the effective HS fraction as $\gamma_{\text{HS}} = (\gamma'_{\text{HS}} - \gamma_f) / (\gamma_i - \gamma_f)$, where γ'_{HS} corresponds to the measured HS fraction. Then by substituting the effective HS fraction into Eq. (1) we can derive Eq. (3) as follows:

$$\frac{d\gamma'_{\text{HS}}}{dt} = -\frac{1}{\tau'} \exp\left[\alpha\left(0.5 - \frac{\gamma'_{\text{HS}}}{\gamma_i - \gamma_f}\right)\right] (\gamma'_{\text{HS}} - \gamma_f). \quad (3)$$

where $\tau' = \tau \exp[-\alpha\gamma_f / (\gamma_i - \gamma_f)]$ means an inverse of $k(\gamma_{\text{HS}})$ at $\gamma_{\text{HS}} = (\gamma_i - \gamma_f) / 2$. Equation (3) is in a fairly good agreement with the observed relaxation curves with τ' and α as free parameters, as shown in Figs. 1(b) and 1(c), implying that the cooperative interactions between the molecules play

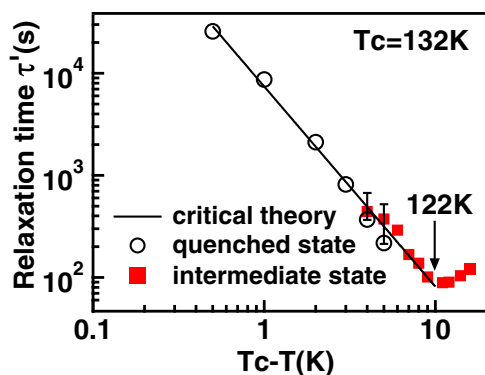


FIG. 2. (Color online) Temperature dependence of the relaxation time in the quenched state (closed square) and the intermediate state (open circle) on a logarithmic scale. The solid line is the best-fit curve according to Eq. (4) with $T_c = 132 \pm 0.2$ K and $\Delta = 2.0 \pm 0.5$.

an important role in $[\text{Fe}(\text{ptz})_6](\text{BF}_4)_2$. The acceleration factors α of relaxation curves [Figs. 1(b) and 1(c)] are determined to be 3.1 ± 0.3 and 3.5 ± 0.4 , respectively, and this values are bigger than the value of $\alpha \approx 2$ predicted by the relaxation curves below 60 K.²⁷ We think that this difference is due to the experimental temperature because it is reported that the acceleration factor in $\text{Fe}(\text{PM-BiA})_2(\text{NCS})_2$ complex near the thermal transition temperature is different from that below the light induced excited spin state trapping (LIESST) temperature.²⁸

In Fig. 2, we plot the relaxation times τ' for the quenched state and the intermediate state as a function of the reduced temperature $T_c - T$. The relaxation time diverges at a certain temperature, T_c above 122 K. According to the theory of dynamical critical phenomena,²⁹ the temperature dependence of the relaxation time in the vicinity of the critical temperature can be described as follows:

$$\tau' \propto \frac{1}{(T_c - T)^\Delta}, \quad (4)$$

where T_c is the critical temperature and Δ is the dynamical critical exponent. We estimate T_c and Δ to be 132 ± 0.2 K and 2.0 ± 0.5 , respectively. The phase-transition phenomena in spin-crossover complexes are theoretically discussed within the framework of the Ising-type model.³⁰ The obtained value of the dynamical critical exponent $\Delta = 2.0 \pm 0.5$ is close to the calculated values 1.75 and 1.25 derived from the two- and three-dimensional Ising model, respectively.³¹

In order to clarify the structure of the intermediate and PIHS state, we measured the IR absorption spectra in the different states using a Bruker optics Fourier transform infrared (FTIR) spectrometer (VERTEX 80v) and microscope system (HYPERION). As shown in Fig. 3, the IR spectra of the PIHS state at 116 K and the intermediate state at 125 K have almost the same peaks at 1800 and 1825 cm^{-1} as that of the thermal HS state with HT structure at 140 K. In the slow-cooled LS state at 116 K, the two peaks disappear and the specific peak emerges at 1780 cm^{-1} . Thus, these three peaks (1780, 1800, and 1825 cm^{-1}) are makers of the different states: LS, HS, and HT structure states, respectively.

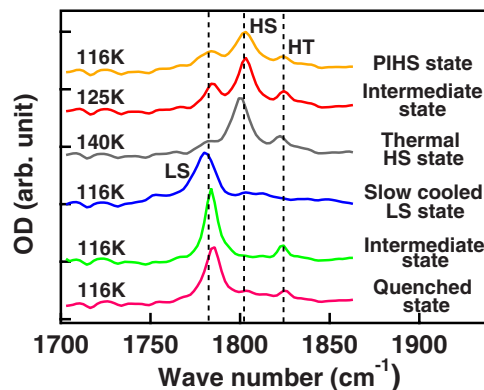


FIG. 3. (Color online) Infrared-absorption spectra in the PIHS state under the laser irradiation (116 K), in the intermediate state (116 and 125 K), in the thermal HS state (140 K), in the slow cooled LS state (116 K), and in the quenched state (116 K).

Then, the IR spectrum of the intermediate state at 116 K has the same peaks at 1780 (LS) and 1825 cm^{-1} (HT) as that of the quenched state at 116 K. Therefore, the structure of the intermediate and quenched state is confirmed as the HT structure even in the LS state by the FTIR spectra.

Figure 4(a) shows the temperature dependence of the HS fraction in the quenched state and the intermediate state. The quenched state was created by rapidly cooling the sample (>50 K/min), and under this cooling condition the spin transition from the HS to LS state occurs without the crystallographic phase transition.¹⁶ We measured the temperature dependence of the HS fraction in the quenched state by increasing the temperature at the rate of 10 K/min, as shown in Fig. 4(a). The spin transition is observed at 122 K, and the LS to HS transition temperature is different from that observed (137 K) when the LS state was obtained by slowly cooled (1 K/min). Also, comparing the temperature dependences between the intermediate and quenched states in Fig.

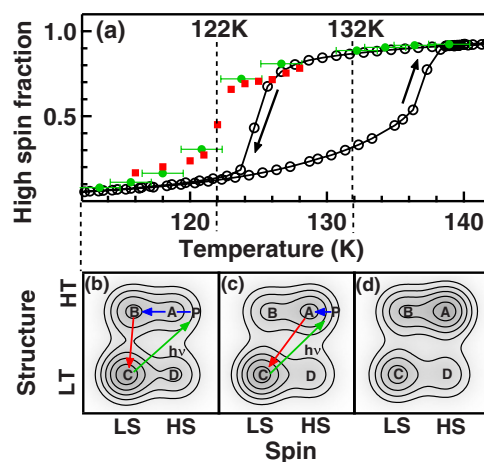


FIG. 4. (Color online) (a) Temperature dependence of the HS fraction in the intermediate state (closed square), in the quenched state (10 K/min) (closed circle), and upon slow temperature change in the dark (1 K/min) (open circle). [(b)–(d)] Proposed contour plot of the potential energy of structure and spin parameters (b) below 122 K, (c) between 122 and 132 K, and (d) above 132 K.

4(a), their behaviors are quite similar and their spin transition temperatures (122 K) are nearly the same. Hence, the IR spectra in Fig. 3 and the temperature dependence of HS fraction in Fig. 4(a) confirm that the intermediate state is the same as the quenched state.

In order to realize the relation between the phase transitions with competing order parameters and their relaxations, we propose a qualitative picture of the potential energy depending on temperature. Figures 4(b)–4(d) show the schematic figure of category plot of the potential energy. The horizontal and longitudinal axes show the spin and structural orders, respectively. There are four local minimum points A, B, C, and D. Above 132 K the true ground state is A (HS-HT), as shown in Fig. 4(d). At 132 K the true ground state is changed from A to C (LS-LT) and the crystallographic phase transition accompanied by the spin transition occurs as shown Figs. 4(c) and 4(d). The photoexcitation induces the transition from C to the PIHS state P (HS-HT). Between 122 and 132 K, P first relaxes to the intermediate state A and then relaxes to the true ground state C as shown in Fig. 4(c). As a result, in this temperature region the spin and structural transitions are coupled. Below 122 K, B (LS-HT) becomes more stable than A, and the spin transition with the HT structure (A → B) may be activated. As shown in Fig. 4(b), P first relaxes to the intermediate state B and then relaxes to the true ground state C. Therefore, in this temperature region the spin and structural transitions are decoupled. At 122 K the lifetime of the intermediate state becomes minimum as shown in Fig. 2, implying that both A and B are unstable.

Therefore the plateau region of intermediate state indicated by the arrows in Fig. 1(c) seems to be vanished.

In conclusion, we have studied the relaxation dynamics in $[\text{Fe}(\text{ptz})_6](\text{BF}_4)_2$ using time-resolved magnetic-susceptibility and optical-absorption measurements. We observed two-step relaxations of the PIHS state from the HS to LS state through an intermediate state. The temperature dependence of the HS fraction and the IR-absorption spectra show that the intermediate state is the same as the quenched state and that a spin transition in the intermediate state occurs at 122 K without a crystallographic phase transition (HS-HT ↔ LS-HT). Furthermore, the critical slowing down phenomena clearly indicates that the crystallographic phase transition with the spin transition occurs at 132 K (HS-HT ↔ LS-LT).

This work was supported by a Grant-in-Aid for Creative Scientific Research program (Grant No. 18GS0208) from the Ministry of Education, Culture, Sports, Science and Technology (MEXT) of Japan and by a Grant-in-Aid for Scientific Research on Innovative Areas “Optical science of dynamically correlated electrons (DYCE)” (Grant No. 20104007) of the Ministry of Education, Culture, Sports, Science and Technology (MEXT, Japan). The authors also acknowledge financial support from the FASTSWITCH ANR project and a Grant-in-Aid for the Global COE Program “The Next Generation of Physics, Spun from Universality and Emergence” from the Ministry of Education, Culture, Sports, Science and Technology (MEXT) of Japan.

*kochan@scphys.kyoto-u.ac.jp

¹S. Koshihara, Y. Tokura, K. Takeda, and T. Koda, *Phys. Rev. Lett.* **68**, 1148 (1992).

²K. Miyano, T. Tanaka, Y. Tomioka, and Y. Tokura, *Phys. Rev. Lett.* **78**, 4257 (1997).

³S. Koshihara *et al.*, *J. Phys. Chem. B* **103**, 2592 (1999).

⁴Y. Ogawa *et al.*, *Phys. Rev. Lett.* **84**, 3181 (2000).

⁵*Photoinduced phase transitions*, edited by K. Nasu (World Scientific Publishing, Singapore, 2004).

⁶L. H. Böttger *et al.*, *Chem. Phys. Lett.* **429**, 189 (2006).

⁷J. Jeftić and A. Hauser, *J. Phys. Chem. B* **101**, 10262 (1997).

⁸A. Hauser *et al.*, *Coord. Chem. Rev.* **190-192**, 471 (1999).

⁹I. Krivokapic, C. Enachescu, R. Bronisz, and A. Hauser, *Inorg. Chim. Acta* **361**, 3616 (2008).

¹⁰Y. Tokura, *Science* **312**, 1481 (2006).

¹¹M. Matsubara *et al.*, *J. Appl. Phys.* **103**, 07B110 (2008).

¹²H. Kamioka, Y. Moritomo, W. Kosaka, and S. Ohkoshi, *Phys. Rev. B* **77**, 180301(R) (2008).

¹³E. Collet *et al.*, *Science* **300**, 612 (2003).

¹⁴M. Chollet *et al.*, *Science* **307**, 86 (2005).

¹⁵A. Hauser, *Top. Curr. Chem.* **234**, 155 (2004).

¹⁶J. Kusz, P. Gülich, and H. Spiering, *Top. Curr. Chem.* **234**, 129 (2004).

¹⁷A. Ozarowski and B. R. McGarvey, *Inorg. Chem.* **28**, 2262 (1989).

¹⁸L. Wiehl, *Acta Crystallogr., Sect. B: Struct. Sci.* **49**, 289 (1993).

¹⁹N. Ould Moussa *et al.*, *Chem. Phys. Lett.* **402**, 503 (2005).

²⁰J. Jeftić, R. Hinek, C. Capelli, and A. Hauser, *Inorg. Chem.* **36**, 3080 (1997).

²¹Y. Moritomo *et al.*, *J. Phys. Soc. Jpn.* **71**, 1015 (2002).

²²Y. Moritomo *et al.*, *J. Phys. Soc. Jpn.* **71**, 2609 (2002).

²³P. L. Franke, J. G. Haasnoot, and A. P. Zuur, *Inorg. Chim. Acta* **59**, 5 (1982).

²⁴S. Decurtins *et al.*, *Inorg. Chem.* **24**, 2174 (1985).

²⁵We measured IR spectra under the laser irradiation. The temperature dependence of the peak position of the HS state around 1800 cm^{-1} induced by the laser irradiation is different from that of the thermal HS state. This directly indicates that the PIHS state is not the thermal HS state created by the laser heating effect [Fig. 1(c)].

²⁶The possible reason of such a sigmoidal relaxation curve is the spatial inhomogeneity due to the domain creation [see F. Varret *et al.*, *EPL* **77**, 30007 (2007)] or defects.

²⁷A. Hauser, *Chem. Phys. Lett.* **192**, 65 (1992).

²⁸J. Degert *et al.*, *Chem. Phys. Lett.* **415**, 206 (2005).

²⁹P. C. Hohenberg and B. I. Halperin, *Rev. Mod. Phys.* **49**, 435 (1977).

³⁰A. Bousseksou *et al.*, *J. Phys. I* **2**, 1381 (1992).

³¹Z.-D. Zhang, *Philos. Mag.* **87**, 5309 (2007).